# Super Robust, Anti-Bacterial Polyurethane Ionogel with High Sensitivity and Hydrophobicity

by

Wei Wang,[1,3] Shiyang Yan,[1,3] Yihong Zhao,[1,3] Hao Liu,[1,3] Luming Yang[1,2,3*] and Biyu Peng[1,2,3*]

[1]*National Engineering Research Center of Clean Technology in Leather Industry, Sichuan University*, Chengdu 610065, China.

[2]*Key Laboratory of Leather Chemistry and Engineering of Ministry of Education, Sichuan University,* Chengdu 610065, China.

[3]*College of Biomass Science and Engineering, Sichuan University*, Chengdu 610065, China.

## Abstract

Ionogel based on ionic liquids plays a vital role in wearable electronic devices. In this study, a robust and anti-bacterial ionogel with high sensitivity and hydrophobicity is synthesized by adding 1-ethyl-3-methylimidazolium bis(trifluoromethylsulfonyl)imide to thermoplastic polyurethanes at a ratio of 1:1. The ionogel not only demonstrates tensile strength of 23.1 MPa and elongation at break of 1008%, but also exhibits excellent fatigue resistance with low residual strain (8%) and small hysteresis loop. Ionic liquid makes the ionogel have high-temperature stability ($T_{5\%}$ near 300°C) and low $T_g$ (-63.3°C). Due to the anti-bacterial property of ionic liquid, the ionogel formed by ionic liquid has anti-bacterial property, with up to 99% inhibition against *E. coli* and *S. aureus*. The sensor prepared with the ionogel shows a *Gauge Factor* of 1.8, with a short response time (128 ms) and a stable induction signal under water and at low temperature. Due to those performance characteristics, we believe that the study could provide insights for subsequent research on ionogel-based wearable electronic devices, for instance, the development of electronic skin in the leather industry.

## Introduction

Nowadays, wearable electronic devices have received considerable attention due to their flexibility and stretchability, and have made significant progress in various fields, such as human movement and health monitoring,[1-3] electronic skin[4-6] and human-computer interaction interfaces.[7-9] However, the severe conditions encountered in practical applications, such as extreme temperature, dryness, humidity, and underwater environments; limit the research on flexible sensors. At present, hydrogel is most widely used in the field of wearable electronic devices because of its high conductivity, superb stretchability, and bio-tissue-like moduli.[10-14] However, due to its high-water content characteristic, hydrogel faces two challenges which must be overcome in practical applications. One is that hydrogel would freeze at low temperature, resulting in hardening. The other is that during the long-term use of hydrogel, the solvent water in hydrogel would evaporate, causing it to dry and crack. To address the two challenges mentioned above, a number of strategies have been developed, such as introducing low vapor pressure solvents glycerol[10, 15-18] and organic solvents.[19-21] However, those strategies may increase the risk of adverse reactions through skin contact.

Ionogel has a three-dimensional polymeric network structure that can be combined with ionic liquid (IL), a green and harmless solvent composed of large-sized anions and cations.[22-24] In practical use, IL has excellent electrical conductivity, low freezing point, low vapor pressure and non-toxic properties, which provide ionogel with electrical conductivity and maintains stability in extremely low-temperature environments for long-term use.[25-30] The selection of polymer materials should have good compatibility with IL and require sufficient mechanical property suitable for the intended applications. For instance, Lee et al.[31] combined poly(vinylidene fluoride-co-hexafluoropropylene) (P(VDF-co-HFP)) with 1-butyl-3-methylimidazolium bis[(trifluoromethyl)sulfonyl]imide ([BMI][TFSI]) and 1-butyl-3-methylimidazolium hexafluorophosphate ([BMI][$PF_6$]) to prepare ionogel. Although ionogel has outstanding electrical conductivity and environmental stability, it lacks in some mechanical properties, the tensile strength of which is only about 1.8 MPa. In contrast, thermoplastic polyurethanes (TPU) are polymers with preeminent mechanical properties. According to the report, the polarity of the polyurethane (PU) chain segment makes the TPU highly compatible with ILs.[33] Therefore, it can be speculated that if the mechanical properties of TPU could combine with the electrical conductivity of ILs, ionogel can be obtained with long-lasting fatigue resistance, thus ensuring the stability of the ionogel sensor. In daily use, the ionogel sensor inevitably encounters wet environments or underwater conditions, which affects the sensing performance of most ionogels. Similarly, choosing hydrophobic IL when preparing ionogels can not only make ionogels enhance its hydrophobicity but also avoid interference from wet environments or water molecules in the process of use.[34-36]

Leather is a traditionally natural material obtained from animal skin. Although leather inherits the complex structure and flexibility of the original skin, it lacks the essential sensory ability of the skin. The layered structure of natural leather can load and carry

*Corresponding author email: pengbiyu@scu.edu.cn ; ylmll1982@126.com

Manuscript received June 21, 2023, accepted for publication October 3, 2023.

other materials. Specifically, leather can be considered a potential candidate for manufacturing high-performance electronic skin. For instance, electronic skin can be sprayed with the conductive gel described above at different monitoring points. After that, a conductive circuit can be designed by spreading the conductive silver paste to form the sensing points of various signals, such as pressure, temperature, etc. As a result, combining leather with functional materials allows leather to restore the sensing characteristics of natural skin.

In the study, we have explored a preparation process of ionogel with sensing properties. To be specific, we chose a TPU elastomer with sufficient mechanical properties and hydrophobic IL to prepare ionogel. The prepared ionogel is expected to inherit the characteristics of TPU and IL, such as mechanical properties, electrical conductivity and hydrophobicity, so as to ensure the reliability of ionogel with stable mechanical property and sufficient conductivity in practical applications. Due to ionogel's hydrophobicity, the application range of ionogel can be extended to cope with complex humid environment in practical use. In general, the study not only demonstrates ionogel's structure and mechanical properties in detail, but also discusses the anti-bacterial property and environmental stability of ionogel. After the sensor is made, the research steps into sensitivity, sensing stability, and underwater sensing performance of ionogel.

## 2. Experimental

### 2.1 Materials

ILs 1-ethyl-3-methylimidazolium dicyanamide ([EMIM][DCA]), 1-ethyl-3-methylimidazolium bis(trifluoromethylsulfonyl)imide ([EMIM][TFSI]), and 1-ethyl-3-methylimidazolium tetrafluoroborate ([EMIM][$BF_4$]), were purchased from Monils Chemicals (Shanghai) Co., Ltd (Shanghai, China). TPU was obtained from DuPont. Methyl ethyl ketone (MEK) was provided by Chengdu KeLong Reagents Co.

### 2.2. Preparation of TPU/IL ionogel

In order to select the most suitable IL to combine with TPU to obtain the ionogel with better mechanical property, TPU was mixed with different types of ILs in various solvents and eventually dried to get ionogel. After choosing the most effective IL by the above process, TPU and IL were mixed in MEK at ratios of 4:1, 2:1, and 1:1. Then, the obtained ionogel was dried out and named as TPU/IL-4:1, TPU/IL-2:1, and TPU/IL-1:1 respectively. Since the thickness of ionogel was around 100 μm, Silver (Ag) electrode could connect to both ends of ionogel to create a strain sensor.

### 2.3 Characterization

A Perkin-Elmer FTIR spectrometer was employed to acquire the Fourier transform infrared (FT-IR) spectra. A UV-1800 spectrophotometer (Shimadzu) was utilized to collect the UV-visible transmittance spectra. The morphology and structure of ionogel were observed using a field emission scanning electron microscope (XL-30 ESEM FEG microscope, FEI Company). A potentialstat with alternating current (AC) was used for impedance spectroscopy (Princeton, PARSTAT MC) to determine the ionic conductivity ($\sigma_i$) of the ionogel. A tensile test machine (Instron 4465) was used to analyze the mechanical properties and resilience of the ionogel with a stretching rate of 20 mm $min^{-1}$. A Q800 (TA Instrument) was used to carry out dynamic mechanical analysis (DMA) by testing the temperature dependence of G′ and G″ with a heating rate of 3°C/min and a frequency of 1 Hz. The digital images were captured using a Nikon D7100 camera. Hangzhou LinkZill Technology Co., Ltd. supported the wireless system. *S. aureus* ATCC 6538 and *E. coli* ATCC 25922 were incubated in nutrient broth at 37°C for 16 hours and diluted in nutrient broth to yield a density of $1 \times 10^6$ cfu/mL. Different concentration of TPU or TPU/IL-1:1 solution was incubated with the bacterial suspension for 24 hours, after which an aliquot of 200 μL of the samples was aspirated to measure $OD_{600}$ at regular intervals. In addition, 10 μL of the bacterial suspension was spotted at intervals on nutrient agar plates along with the samples and incubated at 37°C for 24 hours for visualization of the anti-bacterial effect, which was recorded with a camera.

## 3. Results and Discussions

### 3.1 Preparation and structure of the ionogels

After combining different types of ILs with TPU, compatible raw materials with stable ionogel were selected. In subsequent studies, different proportions of TPU were mixed with IL [EMIM][TFSI] in MEK and dried to form homogeneous ionogel. The preparation process of ionogel is shown in Figure 1. The ionogel with different proportions was characterized by FT-IR, as shown in Figure

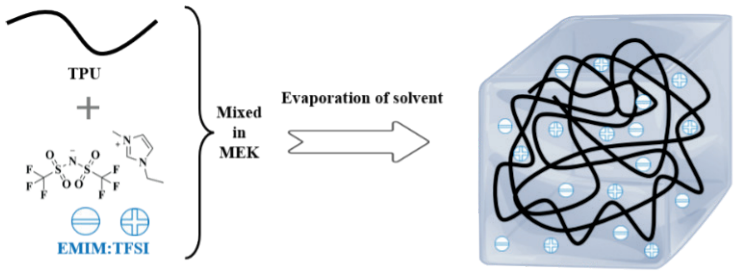


**Figure 1.** The preparation process of the ionogel

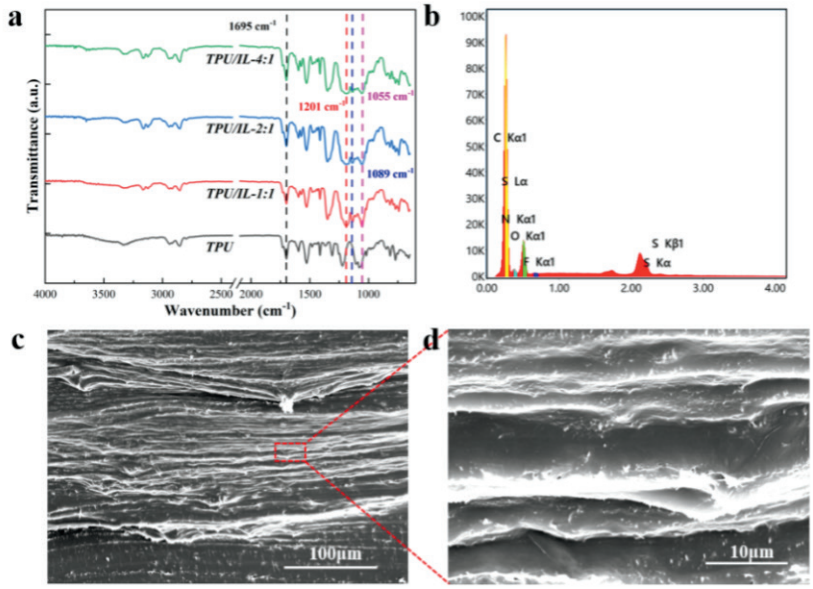


**Figure 2.** The characterization of TPU/IL ionogel: **(a)** FT-IR spectrum; **(b)** EDS analysis of the ionogel TPU/IL-1:1; **(c)** SEM photo of ionogel TPU/IL-1:1; **(d)** Localized enlargement of the SEM photo

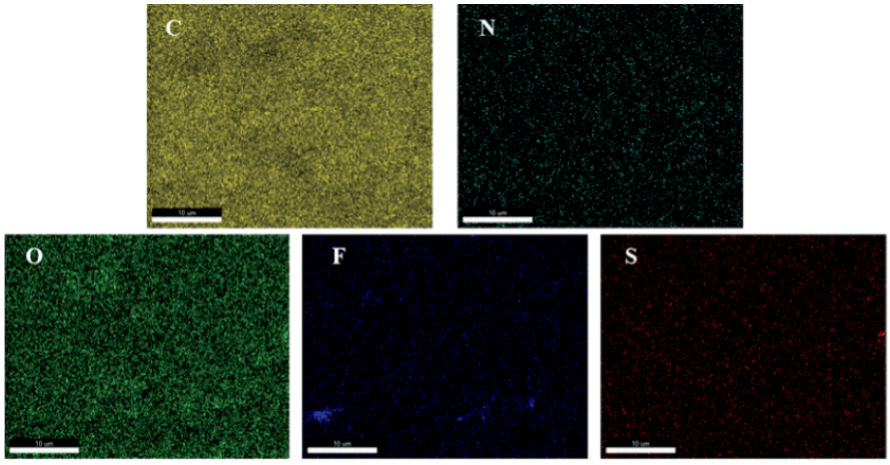


**Figure 3.** The EDS analysis of TPU/IL-1:1

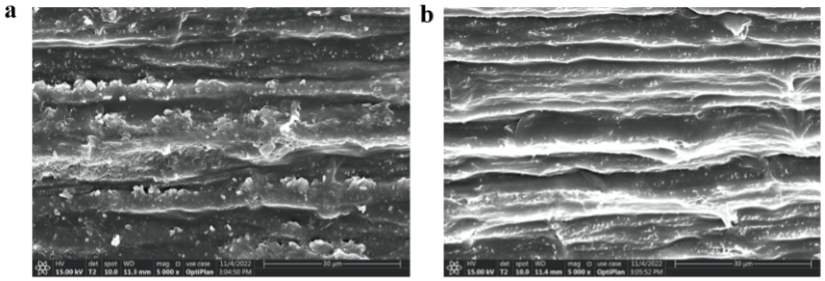


**Figure 4.** The SEM photo of **(a)** TPU/IL-4:1 and **(b)** TPU/IL-2:1

2a. It was obvious that the characteristic absorption peak 37 belonging to polyurethane (1695 $cm^{-1}$) and IL [EMIM][TFSI] (the characteristic absorption peak of S-N-S, S=O, and C-F are located at 1055 $cm^{-1}$, 1198 $cm^{-1}$, and 1201 $cm^{-1}$) appeared in the IR-spectra of ionogel.[37] The microstructure of the prepared ionogel was observed by SEM and EDS. The EDS analysis of TPU/IL-1:1 ionogel, shown in Figure 2b and Figure 3, demonstrated that C, N, O, S, and F elements in IL were evenly distributed in the gel system. As shown in Figures 2c, 2d, 4a, and 4b, a great number of microscopic channels can be found inside the prepared ionogel, used for conductive ion transport in IL when energized. Also, the pore size and number of the microscopic channels increase with the increasing ratio of IL. As a result, it indicates that the ionogel has been successfully prepared.

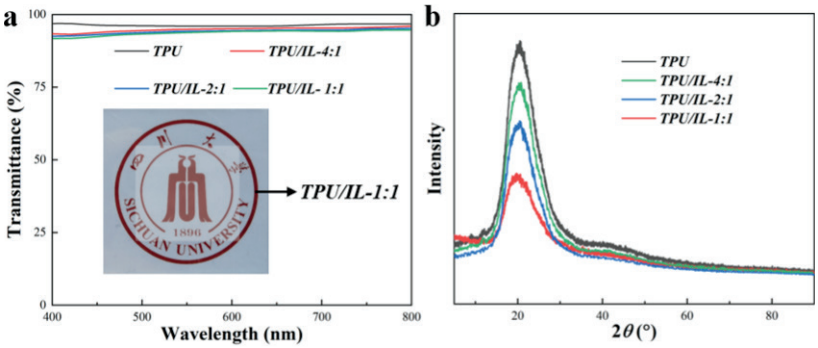


**Figure 5.** The structural characterization of TPU/IL ionogel: **(a)** Transmittance of ionogel (the inserted photo is the TPU/IL-1:1 on the top of the university logo); **(b)** XRD spectra

As shown in Figure 5a, all ionogel maintained a transmittance of above 90% in the visible light zone. Taking TPU/IL-1:1 as an example, it was placed on the top of the emblem of Sichuan University. The emblem could still be clearly seen through the ionosphere. The XRD results shown in Figure 5b indicated that with the increase of IL content, the crystalline part between the hard segments in the original TPU was gradually dissolved or partially dissolved. The peak intensity of the crystal was also gradually weakened at the same time. Therefore, it reflected the transmittance and crystallinity of ionogel.

### 3.2 Stretchability of the ionogels

As shown in Figure 6a, the mechanical property of TPU/IL-X was measured by tensile test. With the addition of IL [EMIM][TFSI] loading, the tensile strength of ionogel decreased, while the fracture strain increased at first and then decreased after adding IL. From TPU to TPU/IL-1:1, the tensile strength of the sample ranged from 55.4 MPa to 23.1 MPa, and the fracture strain varied approximately from 888% to 1037%, as shown in Figures 6b and 6c. The above mechanical behavior may be related to the swelling or dissolution ability of IL on TPU, thereby reducing micro-phase separation and crystallization of PU chains.[38, 39] To verify the mechanical durability of ionogel, each prepared material was subjected to 50% strain by continuous tensile tests, as shown in Figure 6d, Figure 7a, and Figure 7b. After ten repeated tensile tests, all samples exhibited a large hysteresis curve. Except for the residual strain of about 8% in the first cycle, the tensile strength decreased slightly in the rest of the nine tensile cycles. The hysteresis curve of ionogel was slight, with only about 4% of residual strain. The above results could be attributed to the irreversible fracture of some cross-linked points in ionogel during the first tensile process, which could not be recovered during the relaxation process. Therefore, it showed a slight decrease in strength in subsequent stretches. Since the combined effect of ionic bonds and hydrogen bonds in ionogel allowed to maintain constant tensile strength in the following nine tensile cycles, a slight hysteresis curve and reduced residual strain were observed.

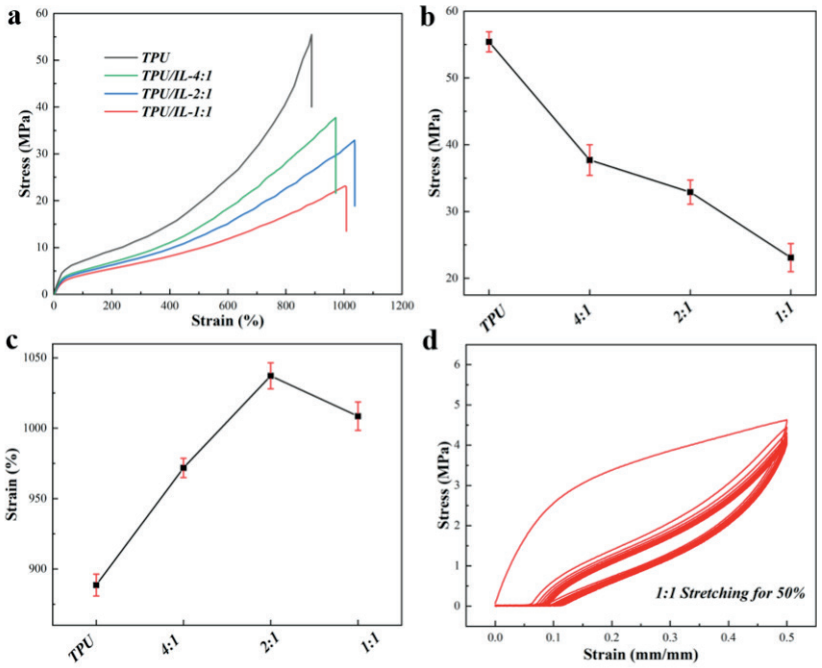


**Figure 6.** Stretchability of ionogel: **(a)** Stress-strain curves of ionogel with different types of ILs; **(b)** Stress data of stress-strain curves; **(c)** Strain at break data of stress-strain curves; **(d)** Different strains exerted on TPU/IL-1:1 by subsequent tensile tests

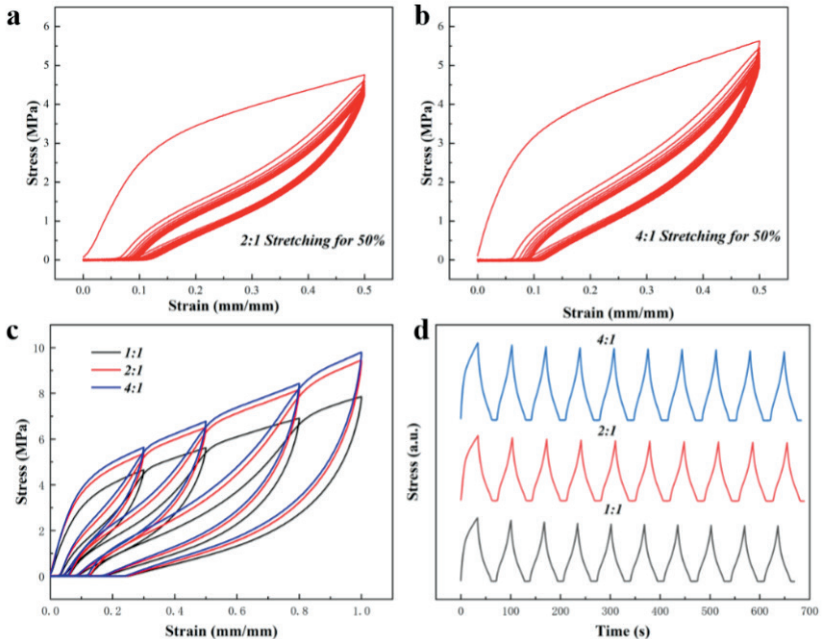


**Figure 7.** **(a)** The ten cyclic tensile tests TPU/IL-2:1; **(b)** The ten cyclic tensile tests TPU/IL-4:1; **(c)** Cyclic stretching with three ratios of different stretching rates; **(d)** Ten times tensile strength change of the same tensile rate

What is more, the tensile strength and cycle number curves, as shown in Figures 7c and 7d, indicated that all ionogel samples had stable mechanical properties, which in turn led to the expectation that, with satisfactory stretchability, the prepared ionogel could meet the functional requirements of wearable devices.

### 3.3 Environmental stability of the ionogels

In order to verify whether ionogel has good environmental stability, we have tested ionogel's thermal stability characterized by thermogravimetric analysis (TGA). As shown in Figure 8a, ionogel had a thermal stability of $T_{5\%}$ close to 300°C. After that, TPU/IL-1:1 was placed in an open fume hood for one month and showed little quality change during the evaluation period, as shown in Figure 8b. The above experimental results showed that the prepared ionogel had proper environmental stability and maintained a stable gel state in a heated environment or at room temperature. Moreover, as shown in Figure 8c, we have performed a dynamic mechanical analysis of ionogel to verify its transition temperature. Considering the low freezing point of ILs, ionogel presented a glass transition temperature at -63.3°C, which indicated that ionogel could remain flexible in sub-zero temperatures.

### 3.4 Anti-bacterial property of the ionogels

As IL has certain anti-bacterial properties,[40, 41] ionogel made of IL and TPU is expected to inherit some degree of bactericidal reactions. The experiment we did was evaluated with two common bacterial strains, including *S. aureus* and *E. coli*. As shown in Figure 9, the inhibition circle increased with the increase of IL content. To further investigate the inhibition effect of TPU/IL-1:1 against bacteria, we co-cultured ionogel with each microorganism to observe its survival rate, shown in Figures 10a and 10b. After 24 hours of co-incubation, the growth of both bacteria was inhibited,

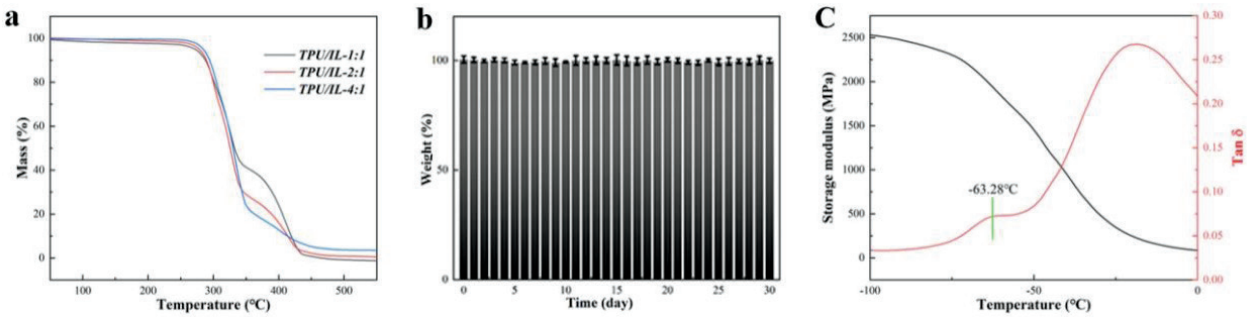


**Figure 8.** Environmental stability of ionogel: **(a)** TGA; **(b)** The mass changes of TPU/IL-1:1 in an open fume hood over one month; **(c)** DMA of TPU/IL-1:1

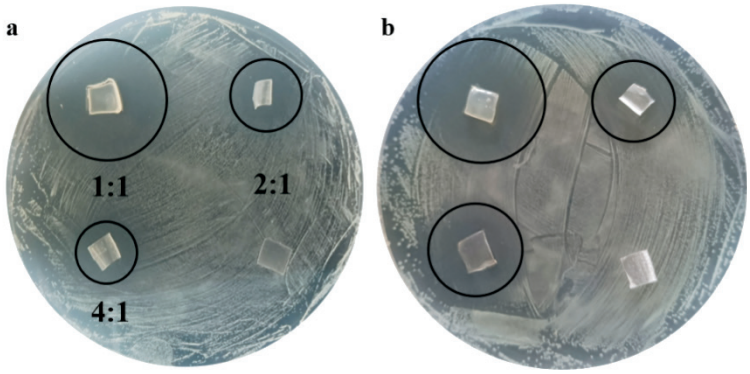


**Figure 9.** The inhibition circle of the ionogel with different IL contents against two bacteria: **(a)** *S. aureus*; **(b)** *E. coli*

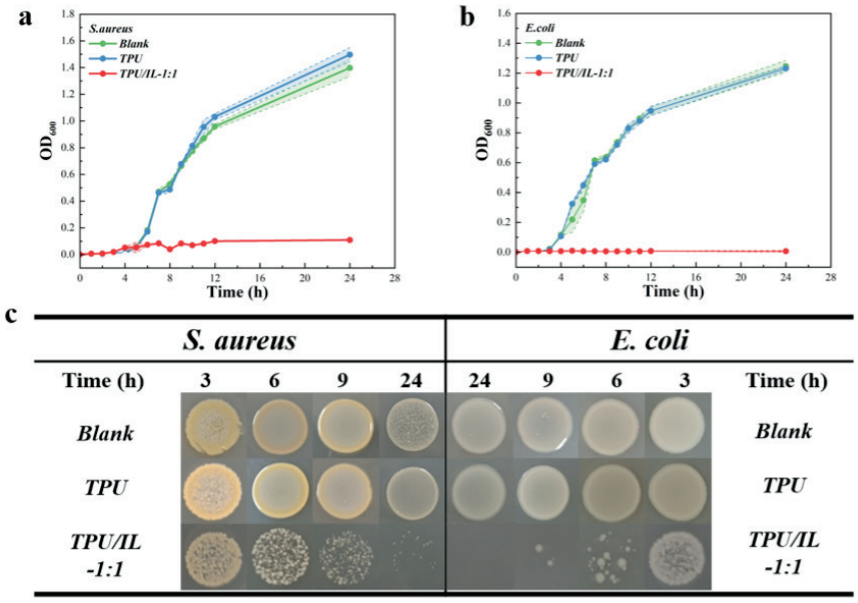


**Figure 10.** Anti-bacterial property of TPU/IL-1:1: **(a)** *S. aureus*; **(b)** *E. coli*; **(c)** Lithographs at different co-cultured sampling times.

and the anti-bacterial efficiency of ionogel was maintained above 99% for both microorganisms. Lithographs at different co-cultured sampling times were illustrated in Figure 10c.

### 3.5 The ionogels as strain sensor

As shown in Figure 11a, we measured the ionic conductivity of TPU/IL-4:1 to TPU/IL-1:1 under ambient conditions. The ionic conductivity increased with the increase of IL load from 2.1 S $cm^{-1}$ to 11.8 S $cm^{-1}$, which was related to IL [EMIM][TFSI]. Also, the massive and dense channels inside ionogel facilitated ionic transportation and access to $EMIM^+$ cations.

The sensitivity of the ionogel sensor, expressed as *Gauge Factor* (*GF*), could be obtained from the mathematical fitting of the relative change of resistance ($\Delta R/R_0$) and the strain plot. The relative change of resistance varied with the mechanical strain of the sensor, as shown in Figure 11b. After fitting a straight line in the range of 0% to 150%, the slope of the curve with the variation of $\Delta R/R_0$ was 1.8 in value. Compared to other ionogel sensors reported so far,[42, 43] the prepared ionogel sensor had a relatively high sensitivity and wide sensing range. With the ionogel sensor in five cycles at different elongations with 1%, 5%, 10%, 20%, 50%, and 100%, the signal change of $\Delta R/R_0$ was shown in Figures 11c and 11d. Furthermore, five hundred cycles were performed under 50% stretch in Figure 11e. To be specific, in five hundred uninterrupted load-unloading cycles, the ionogel sensor exhibited elasticity and fatigue resistance, with little change in $\Delta R/R_0$ signal. As shown in Figure 11f, the response time of the ionogel sensor was 128ms.

Because the ionogel sensor had a low glass transition temperature, it could meet the functional requirement in the minus 20 degrees environment. Therefore, the *GF* plot could be measured in sub-zero conditions, as shown in Figure 12a. Since the sensitivity of the ionogel sensor was almost the same as the original condition, the *GF* curve could be fitted to a straight line with a slope of 1.8 even at a temperature of -20°C. As shown in Figures 12b and 12c, the

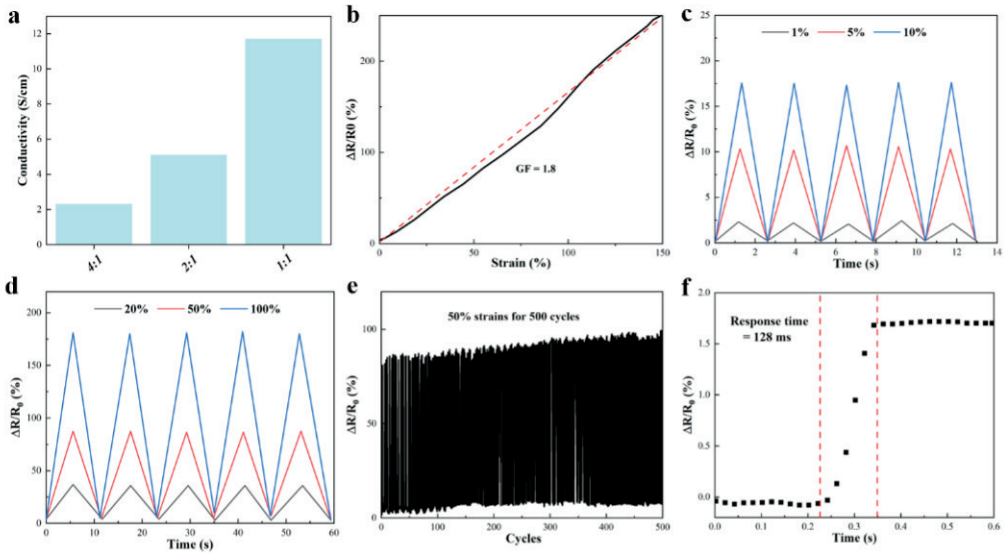


**Figure 11.** The strain property and relationship between stains and electrical resistance: **(a)** Ionic conductivity of ionogel; **(b)** *GF* curve of ionogel sensor; **(c)** Five successive load-unloading cycles at 1% to 10% strain of ionogel sensor; **(d)** Five successive load-unloading cycles at 20% to 100% strain of ionogel sensor; **(e)** 50% strain for 500 cycles; **(f)** Response time.

tensile test of the ionogel sensor was carried out at the same negative temperature of -20°C. The test result showed that the sensing ability ($\Delta R/R_0$ signal) of the ionogel sensor remained stable and could almost replicate the response in its original state.

Based on the hydrophobicity of IL [EMIM][TFSI], the ionogel sensor is expected to have a certain degree of hydrophobicity. In order to prove that the ionogel is hydrophobic, the sensing ability ($\Delta R/R_0$ signal) test of ionogel was conducted underwater. As shown in Figure 12d, the *GF* plot was almost the same as the original state. The variation of the sensing signal also remained stable during the cyclic stretching process, as shown in Figures 12e and 12f.

The above experiments show that the prepared ionogel sensor is not affected by either low temperature or humid environments.

### 3.6 The ionogel as human skin sensor

With the sensing ability for a wide range of strains and different environmental conditions, the ionogel sensor could be used to monitor various movements of the human body. In the following

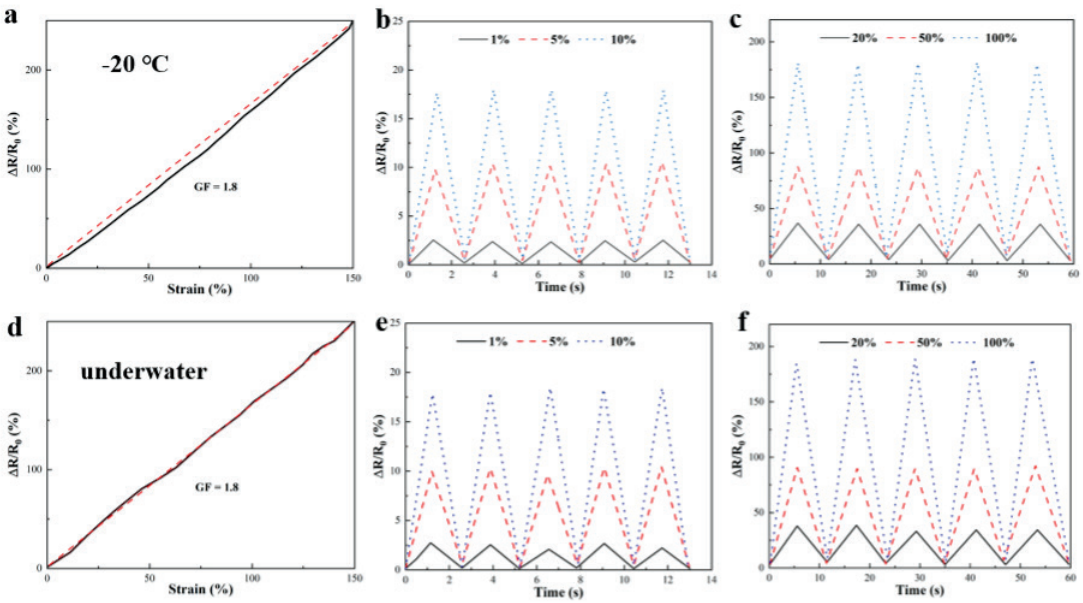


**Figure 12.** The strain property and relationship between stains and electrical resistance: **(a)** *GF* curve of ionogel sensor at -20°C; **(b)** Five successive load-unloading cycles at 1% to 10% strain of ionogel sensor at -20°C; **(c)** Five successive load-unloading cycles at 20% to 100% strain of ionogel sensor at -20°C; **(d)** *GF* curve of ionogel sensor underwater; **(e)** Five successive load-unloading cycles at 1% to 10% strain of ionogel sensor underwater; **(f)** Five successive load-unloading cycles at 20% to 100% strain of ionogel sensor underwater.

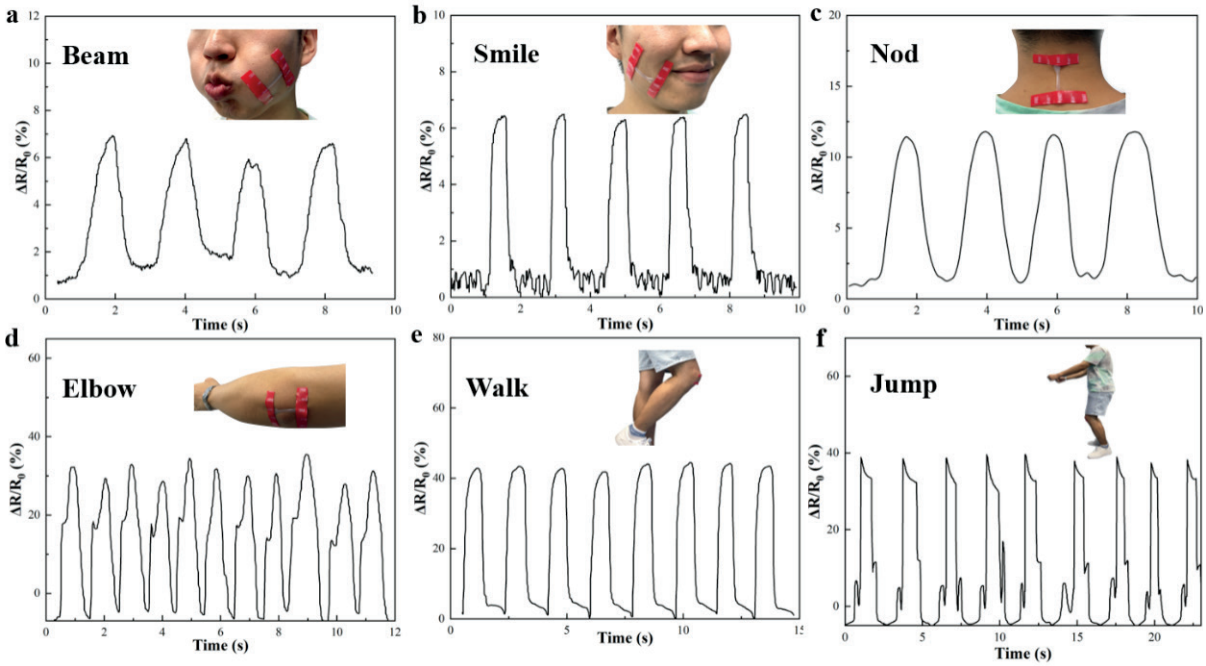


**Figure 13.** Relative resistance changes of TPU/IL-1:1 ionogel for various human movements.
**(a)** Beam; **(b)** Smile; **(c)** Nod; **(d)** Bend elbow repeatedly; **(e)** Walk; **(f)** Jump.

experiment, the ionogel sensor was connected to a wireless system attached to different parts of the human body. Specifically, the wireless system was connected to a mobile phone via Bluetooth to monitor the real-time response of the ionogel sensor's resistance during use. The testing system could accurately detect some subtle facial expressions of the human body, such as beaming and smiling, as shown in Figures 13a and 13b. When the volunteers repeatedly performed facial expressions, the resistance of the ionogel sensor changed with the body movements, corresponding to a regular changing waveform of the mobile application interface. As shown in Figure 13c, as the volunteers bent the neck attached to the ionogel sensor, the application interface displayed the regular waveform accordingly. Unlike the results evaluated in the tensile test in the laboratory, a different waveform could be generated since the deformation of ionogel varied along with the volunteers' movements. In addition, due to the high tensile property of ionogel, large-scale movement signals of human body could even be detected, as shown in Figures 13d, 13e, and 13f. What is more, when the ionogel sensor was attached to the volunteers' elbows and knee joints, the mobile application interface showed large changes in the waveform as the volunteers walked, jumped, or repeatedly bent their elbows.

## 4. Conclusion

The study successfully created a robust ionogel by combining IL with TPU. The prepared ionogel not only has great mechanical property and environmental stability, but also has anti-bacterial property and electrical conductivity. By making it into a sensor, the ionogel possesses adequate sensitivity (*GF*=1.8) and a fast response time of 128ms in the strain range of 0 to 150%. Also, it has stable sensing performance even in sub-zero or underwater environments. What is more, the durability of the ionogel can be explained by the mechanical property of TPU used in its preparation process, while the ionogel's anti-bacterial property and low freezing point characteristics are inherited from the IL test. The introduction of the IL hydrophobicity further endows the ionogel with the ability to work underwater, broadening the application scenario of the ionogel sensor.

In subsequent studies, we will spray the ionogel on leather to produce electronic skin which could respond to external stimuli and make leather materials "alive." Using leather as a base material for flexible and wearable electronics demonstrates a value-added commitment to upgrade cycles for low-value leather. We strongly believe that such a design could not only lead to new flexible electronic products, but also help unlock the potential of multifunctional electronic skin. For instance, a leather insole sensor could monitor the plantar pressure distribution of the diabetic foot to help intervene and treat injuries by understanding patients' body response to the damages.

## Acknowledgments

This work was funded by Science & Technology Department of Sichuan Province (2023YFS0460).

## References


1. Wang, Y., Haick, H., Guo, S., et al.; Skin bioelectronics towards long-term, continuous health monitoring. Chemical Society Reviews, **51**(9), 3759-3793, 2022.
2. Ma, L. Y. and Soin, N.; Recent progress in printed physical sensing electronics for wearable health-monitoring devices: A review. *IEEE Sensors Journal*, **22**(5), 3844-3859, 2022.
3. Du, W., Li, Z., Zhao, Y., et al.; Biocompatible and breathable all-fiber-based piezoresistive sensor with high sensitivity for human physiological movements monitoring. *Chemical Engineering Journal,* **446**, 137268, 2022.
4. Zarei, M., Lee, G., Lee, S. G., et al.; Advances in biodegradable electronic skin: Material progress and recent applications in sensing, robotics, and human–machine interfaces. *Advanced Materials,* **35**(4), 2203193, 2023.
5. Wei, X., Li, H., Yue, W., et al.; A high-accuracy, real-time, intelligent material perception system with a machine-learning-motivated pressure-sensitive electronic skin. *Matter,* **5**(5), 1481-1501, 2022.
6. Xu, J., Wang, H., Du, X., et al.; Self-healing, anti-freezing and highly stretchable polyurethane ionogel as ionic skin for wireless strain sensing. *Chemical Engineering Journal,* **426**, 130724, 2021.
7. Bi, S., Jin, W., Han, X., et al.; Flexible pressure visualization equipment for human-computer interaction. *Materials Today Sustainability*, 100318, 2023.
8. Subba, T. and Chingtham, T. S., A Review on Types of Machine Learning Techniques for Biosignal Evaluation for Human Computer Interaction. *Advanced Computational Paradigms and Hybrid Intelligent Computing: Proceedings of ICACCP 2021*, 457-466, 2022.
9. Vuletic, T., Duffy, A., Hay, L., et al.; Systematic literature review of hand gestures used in human computer interaction interfaces. *International Journal of Human-Computer Studies*, **129**, 74-94, 2019.
10. Li, G., Li, C., Li, G., et al.; Development of conductive hydrogels for fabricating flexible strain sensors. *Small,* **18** (5), 2101518, 2022.
11. Zhang, J., Zhang, Q., Liu, X., et al.; Flexible and wearable strain sensors based on conductive hydrogels. *Journal of Polymer Science,* **60** (18), 2663-2678, 2022.
12. Liu, Y., Wang, L., Mi, Y., et al.; Transparent stretchable hydrogel sensors: materials, design and applications. *Journal of Materials Chemistry C*, **10**(37),13351-13371, 2022.
13. Sharma, A., Ansari, M. Z., Cho, C., Ultrasensitive flexible wearable pressure/strain sensors: Parameters, materials, mechanisms and applications. *Sensors and Actuators A: Physical*, 113934, 2022.
14. Fang, Y., Xu, J., Gao, F., et al.; Self-healable and recyclable polyurethane-polyaniline hydrogel toward flexible strain sensor. *Composites Part B: Engineering,* **219**, 108965, 2021.
15. Zhang, X., Xiang, J., Hong, Y., et al.; Recent Advances in Design Strategies of Tough Hydrogels. *Macromolecular Rapid Communications,* **43** (15), 2200075, 2022.
16. Li, W., Liu, J., Wei, J., et al.; Recent Progress of Conductive Hydrogel Fibers for Flexible Electronics: Fabrications, Applications, and Perspectives. *Advanced Functional Materials,* 2213485, 2023.
17. Hu, L., Chee, P. L., Sugiarto, S., et al.; Hydrogel-Based Flexible Electronics. *Advanced Materials,* **35**(14), 2205326, 2022.
18. Hasan, S., Kouzani, A. Z., Adams, S., et al.; Recent progress in hydrogel-based sensors and energy harvesters. *Sensors and Actuators A: Physical*, **335**, 113382, 2022.
19. Feng, Y., Liu, Z. X., Chen, H., et al.; Functional supramolecular gels based on poly (benzyl ether) dendrons and dendrimers. *Chemical Communications,* **58** (63), 8736-8753, 2022.
20. Jo, Y. J., Ok, J., Kim, S., et al.; Stretchable and soft organic–ionic devices for body-integrated electronic systems. *Advanced Materials Technologies,* **7** (2), 2001273, 2022.
21. Sun, Y., Le, X., Zhou, S., et al.; Recent Progress in Smart Polymeric Gel-Based Information Storage for Anti-Counterfeiting. *Advanced Materials,* **34** (41), 2201262, 2022.
22. De Jesus, S. S. and Maciel Filho, R., Are ionic liquids eco-friendly? *Renewable and Sustainable Energy Reviews,* **157**, 112039, 2022.
23. Qader, I. B. and Prasad, K., Recent developments on ionic liquids and deep eutectic solvents for drug delivery applications. *Pharmaceutical Research,* **39** (10), 2367-2377, 2022.
24. Lu, B., Liu, T., Wang, H., et al.; Ionic liquid transdermal delivery system: Progress, prospects, and challenges. *Journal of Molecular Liquids*, **351**, 118643, 2022.
25. Jamil, R. and Silvester, D. S., Ionic liquid gel polymer electrolytes for flexible supercapacitors: Challenges and prospects. *Current Opinion in Electrochemistry*, **35**, 101046, 2022.
26. Luo, Z., Li, W., Yan, J., et al.; Roles of ionic liquids in adjusting nature of ionogels: A mini review. *Advanced Functional Materials*, **32** (32), 2203988, 2022.
27. Pei, Y., Zhang, Y., Ma, J., et al.; Ionic liquids for advanced materials. *Materials Today Nano,* **17**, 100159, 2022.
28. Wang, S., Jiang, Y., Hu, X., Ionogel-Based Membranes for Safe Lithium/Sodium Batteries. *Advanced Materials*, **34**(52), 2200945, 2022.
29. Wang, H., Qu, M., Zhang, R., et al.; Recent Advances in Flexible, Stretchable, and Self-Healing Sensors. *Flexible and Wearable Sensors: Materials, Technologies, and Challenges*, **81**, 2023.
30. Wen, X., Wang, H., Ren, E., et al.; A robust and sensitive flexible strain sensor based on polyurethane cross-linked composite hydrogels for the detection of human motion. *New Journal of Chemistry*, **46** (40), 19335-19341, 2022.
31. Lee, W. Y., Kim, Y. M., Kwon, J. H., et al.; Correlation between ion gel characteristics and performance of ionic pressure sensors. *Journal of Materials Chemistry C,* **9** (16), 5445-5451, 2021.
32. Hu, Q., Nag, A., Zhang, L., et al.; Reduced graphene oxide-based composites for wearable strain-sensing applications. *Sensors and Actuators A: Physical*, 113767, 2022.
33. Luo, T., Jiao, C., Chen, X., et al.; Flame-retardant effect of modified molecular sieve by ionic liquid in TPU. *Journal of Thermal Analysis and Calorimetry,* **147** (6), 4141-4150, 2022.
34. Wei, J., Xiao, P., Chen, T., et al.; Water-Resistant Conductive gels toward Underwater Wearable Sensing. *Advanced Materials*, 2211758, 2023.
35. Clement, N. and Kandasubramanian, B., 3D Printed Ionogels In Sensors. *Polymer-Plastics Technology and Materials*, **62**(5), 632-654, 2022.

36. Xu, J., Wang, H., Wen, X., et al.; Mechanically Strong, Wet Adhesive, and Self-Healing Polyurethane Ionogel Enhanced with a Semi-interpenetrating Network for Underwater Motion Detection. *ACS Applied Materials & Interfaces,* **14** (48), 54203-54214, 2022.
37. Yuan, C., Zhu, X., Su, L., et al.; Preparation and characterization of a novel ionic conducting foam-type polymeric gel based on polymer PVdF-HFP and ionic liquid [EMIM][TFSI]. *Colloid Polym Science*, **293**, 1945-1952, 2015.
38. Behera, P. K., Mondal, P., Singha, N. K., Polyurethane with an ionic liquid crosslinker: a new class of super shape memory-like polymers. *Polymer chemistry,* **9** (31), 4205-4217, 2018.
39. Gao, R., Zhang, M., Wang, S. W., et al.; Polyurethanes Containing an Imidazolium Diol-Based Ionic-Liquid Chain Extender for Incorporation of Ionic-Liquid Electrolytes. *Macromolecular Chemistry and Physics,* **214** (9), 1027-1036, 2013.
40. Wang, H. L., Wang, Y. X., Liang, Z. H., et al.; Endogenous Ionic-Liquid-Infused Coatings by Phase Separation for Anti-Icing and Anti-Bacterial Applications. *Advanced Materials Interfaces,* **9** (13), 2102570, 2022.
41. Liu, B., Fu, R., Duan, Z., et al.; Ionic liquid-based non-releasing antibacterial, anti-inflammatory, high-transparency hydrogel coupled with electrical stimulation for infected diabetic wound healing. *Composites Part B: Engineering,* **236**, 109804, 2022.
42. Sun, J., Lu, G., Zhou, J., et al.; Robust physically linked double-network ionogel as a flexible bimodal sensor. *ACS applied materials & interfaces*, **12** (12), 14272-14279, 2020.
43. Wang, A., Wang, Y., Zhang, B., et al.; Hydrogen-bonded network enables semi-interpenetrating ionic conductive hydrogels with high stretchability and excellent fatigue resistance for capacitive/resistive bimodal sensors. *Chemical Engineering Journal,* **411**, 128506, 2021.